Rapid Filtration Analysis of Nucleotide Binding to Na,K-ATPase†

Natalya U. Fedosova,‡ Philippe Champeil,§ and Mikael Esmann*,‡

Department of Biophysics, University of Aarhus, Ole Worms Allé 185, DK-8000 Aarhus C, Denmark, and Section de Biophysique des Fonctions Membranaires (DBJC/CEA), Unité de Recherche Associée 2096 (CNRS), IFR-46 and LRA-17V (Université Paris-Sud), Centre d'Etudes de Saclay, 91191 Gif-sur-Yvette Cedex, France

Received September 10, 2002; Revised Manuscript Received December 20, 2002

ABSTRACT: Transient kinetic analysis of nucleotide binding to pig kidney Na,K-ATPase using a rapid filtration technique shows that the interaction between nucleotide and enzyme apparently follows simple first-order kinetics both for ATP in the absence of Mg^{2+} and for ADP in the presence or absence of Mg^{2+}. Rapid filtration experiments with Na,K-ATPase membrane sheets may nevertheless suffer from a problem of accessibility for a fraction of the ATPase binding sites. Accordingly, we estimate from these data that for ATP binding in the absence of Mg^{2+} and the presence of 35 mM Na^+ at pH 7.0 at 20 °C, the bimolecular binding rate constant k_{on} is about 30 $\mu M^{-1}\cdot s^{-1}$ and the dissociation rate constant k_{off} is about 8 s^{-1}. In the presence of 10 mM Mg^{2+}, the binding rate constant is the same as that in the absence of Mg^{2+}. For ADP or MgADP the binding rate constant is about 20 $\mu M^{-1}\cdot s^{-1}$ and the dissociation rate constant is about 12 s^{-1}. Results of rapid-mixing stopped-flow experiments with the fluorescent dye eosin are also consistent with a one-step mechanism of binding of eosin to the ATPase nucleotide site. The implication of these results is that nucleotide binding to Na,K-ATPase both in the absence and presence of Mg^{2+} appears to be a single-step event, at least on the time scale accessible in these experiments.

Na,K-ATPase (EC 3.6.1.37), present in the plasma membrane of animal cells, is responsible for the active transport of Na^+ and K^+ at the expense of the energy released from ATP hydrolysis (*1*). An initial step in the reaction cycle of Na,K-ATPase is high-affinity binding of ATP to the enzyme in the presence of Na^+, followed by Mg^{2+}-dependent phosphorylation and ion translocation; in the absence of Mg^{2+}, the initial binding of ATP is reversible. The aim of the present project is to study the kinetics of the nucleotide binding process in detail, with both equilibrium and transient kinetic methods. High-affinity equilibrium nucleotide binding to Na,K-ATPase was first described by Hegyvary and Post (*2*) and Nørby and Jensen (*3*), and a number of subsequent studies have substantiated the finding that each enzymatically active unit, capable of binding a single ouabain molecule, has a single high-affinity site for binding of ATP or ADP in the presence of Na^+ (*4*, *5*). The detailed description, based on direct measurements of nucleotide binding to Na,K-ATPase, would be of great importance for the analysis (and design) of many kinetic experiments with this enzyme, as a significant deal of kinetic information comes from indirect methods (such as fluorescence) whose interpretation is heavily model-dependent. Using transient kinetic filtration analysis of binding and dissociation rates for ATP, ADP, and MgADP, we aimed to answer the question if the interaction between nucleotide and Na,K-ATPase is described by a simple bimolecular reaction. In this case, the ratio of the rate constants for nucleotide dissociation and binding has to be equal to the separately determined equilibrium dissociation constant. We show here that there is indeed a close agreement between the equilibrium dissociation constants determined experimentally and the ratios of the rate constants for binding and dissociation (k^*_{on} and k^*_{off})[1] deduced from time-resolved binding experiments by analysis in terms of a simple bimolecular reaction of the ligand-dependence of the rate constants (the k_{obs} vs [ligand] curve). Nevertheless, there is an apparent quantitative discrepancy, of about 2-fold, between the dissociation rates deduced from this analysis and the ones which can be experimentally measured in time-resolved ligand exchange experiments. However, we solved this experimental puzzle and suggest that reliable values for k_{on} and k_{off} can indeed be derived from the appropriate filtration experiments. In addition, using stopped flow fluorescence, we show that the fluorescent dye eosin also interacts with Na,K-ATPase in a bimolecular fashion analogous to that of the nucleotides. Our findings have implications in terms of the putative reorientation of the Na,K-ATPase cytosolic domains after ATP binding.

EXPERIMENTAL PROCEDURES

Preparation of Na,K-ATPase. Pig kidney microsomal membranes were prepared as outlined in (*6*), treated with SDS (*7*), and purified by differential centrifugation to a specific activity of 28 μmoles per mg protein per min at 37 °C (see ref *6* for experimental details).

Nucleotide Binding Experiments. The techniques employed in the present study include both equilibrium measurements

† The work was supported by the Danish Medical Research Council (Grant No. 52-00-0914) and Aarhus University Science Foundation.

* To whom correspondence should be addressed. Phone: +45 8942 2930. Fax: +45 8612 9599. E-mail: me@biophys.au.dk.

‡ University of Aarhus.

§ Section de Biophysique des Fonctions Membranaires.

[1] Abbreviations: E_1, the protein conformation of Na,K-ATPase predominant in Na^+-containing media; E_2, the protein conformation of Na,K-ATPase predominant in K^+-containing media; FDP, formycin diphosphate; FTP, formycin triphosphate; k_{on}, bimolecular binding rate constant; k_{off}, dissociation rate constant; K_d, equilibrium dissociation constant; k_{obs}, observed rate constant; *I*, ionic strength.

10.1021/bi0268302 CCC: $25.00
Published on Web 03/06/2003

of radiolabeled nucleotide binding and transient kinetic measurements of the nucleotide binding and dissociation rates (*8*). The experiments were all performed at 20 °C in a 10 mM histidine buffer at pH 7.0. One set of experiments were performed in the presence of 10 mM CDTA which effectively prevents catalytic hydrolysis of ATP. Samples of 10 mM CDTA and 10 mM histidine were titrated to pH 7.0 using about 28 mM NaOH, and 7 mM NaCl was added to give a final $[Na^+] = 35$ mM and $[Cl^-] = 7$ mM. In a second set of experiments, performed with 10 mM $MgCl_2$ present, pH was adjusted to 7.0 with about 1 mM HCl, and NaCl was added to give a final $[Na^+] = 35$ mM ($[Cl^-] = 56$ mM). In a third set of experiments (Figure 4, panel B), protonated Tris replaced Na^+. We used [γ-^{32}P]ATP and [^{14}C]ADP with specific radioactivities of about $1.5 \cdot 10^{10}$ and $2 \cdot 10^9$ Bq/mmol, respectively.

Equilibrium Binding Experiments. Equilibrium binding of nucleotides was measured in double-labeling filtration experiments essentially as previously described (*8*−*10*). First, 1 mL of a suspension of Na,K-ATPase in the above buffer at a concentration of 0.01 mg protein/ml (i.e., a concentration 10-fold lower than the one used in ref *8*) was loaded on two stacked Millipore HAWP 0.45 μm filters; the enzyme remained adsorbed on the top filter, while the bottom one served as a control. Second, the filters were manually perfused at a flow rate of about 1 mL/s with two to six 0.5 mL aliquots of a solution containing radiolabeled nucleotides ([γ-^{32}P]ATP from Amersham or [^{14}C]ADP from New England Nuclear), diluted together with [^{3}H]glucose (from New England Nuclear) in the same buffer as that used for the enzyme, so that complete enzyme equilibration with nucleotide was achieved at all nucleotide concentrations. Then, without rinsing, filters were separately counted in 4 mL Packard Filtercount scintillation fluid. The amount of nucleotide bound to the protein was calculated by subtracting from the total amount of nucleotide on the (top) filter (bound plus unbound nucleotide) the amount of unbound nucleotide, trapped in the filter together with the wetting fluid; the amount of unbound nucleotide was considered to be proportional to the amount of [^{3}H]glucose in the same filter.

Time-Resolved Measurement of Nucleotide Binding and Dissociation Rates. To determine nucleotide binding and dissociation rates, a rapid filtration system was used (RFS-4, Bio-logic, France) (*8*, *11*). In all cases, 1 mL of Na,K-ATPase, generally at a concentration of 0.01 mg protein/ml in the same buffer as described above, was loaded onto a single filter.

For binding-rate experiments, the adsorbed ATPase was directly perfused (at a flow rate of 4.5 mL/s) for various periods (ranging between 30 ms and 150 ms) with the same buffer, supplemented with [^{3}H]glucose and radiolabeled nucleotide (at final concentrations of 0.025−0.4 μM), and counted without rinsing. Nucleotide binding was calculated as described above. See refs *12* and *13* for similar binding experiments with different biological membranes.

For dissociation-rate experiments, the filter with the adsorbed ATPase was first manually perfused with 2−4 mL buffer containing [^{3}H]glucose and radiolabeled nucleotide (at a concentration of 1 μM) as described above, to reach equilibrium. Then the adsorbed ATPase, now with radiolabeled nucleotide bound, was perfused for various periods (ranging between 30 ms and 2 s) with a radioactivity-free buffer, supplemented with 0−0.05 mM unlabeled nucleotide (*8*).

Table 1: Equilibrium Dissociation Constants for ATP and ADP at 20 °C in NaCl[a]

$[Na^+]$ (mM)	K_d for ATP (μM)	K_d for ADP (μM)
7 ($I = 15$)	n.d.	1.74 ± 0.15[b]
27 ($I = 56$)	0.27 ± 0.03	0.78 ± 0.20
35 ($I = 64$)	0.25 ± 0.02	0.69 ± 0.11
57 ($I = 87$)	0.17 ± 0.01	0.64 ± 0.14
107 ($I = 137$)	0.32 ± 0.01	0.97 ± 0.16
157 ($I = 187$)	0.33 ± 0.02	1.21 ± 0.12

[a] These data are obtained in 10 mM histidine (pH 7.0) with 10 mM CDTA present and 0.1 mg protein per filter. K_d's are obtained from single-hyperbolic curves such as those given in Figure 1 (see Methods) and are averages of 3−5 independent determinations. [b] In this experiment 2.5 mM CDTA was present.

In the experiments with ADP and MgADP, the specific radioactivity for the nucleotide solutions was about 7-fold lower than for the ATP-solutions. This, together with the lower binding level for ADP than for ATP at a given nucleotide concentration (due to the larger K_d for ADP), resulted in more experimental scatter in the ADP experiments.

Eosin binding and dissociation experiments were performed on a DX 17MV stopped-flow spectrofluorometer (Applied Photophysics). The following settings were used: excitation wavelength 530 nm, slits 10 nm, 550 nm cutoff filter on the emission side. The experiments were performed in a buffer containing 10 mM histidine, 10 mM CDTA, 35 mM Na^+, pH 7.0 (see ref *14* for details). The reaction was initiated by mixing equal volumes of an enzyme-containing solution and of an eosin-containing solution. The enzyme concentration after mixing was 0.1 μM, while the eosin concentration after mixing ranged from 0.05 to 1 μM.

Curve fitting was performed using the ORIGIN 6.0 software (Microcal, Amherst, CA). Parameters derived are given with standard deviations.

RESULTS

Optimization of Experimental Conditions for Nucleotide Binding. Determination of binding levels for nucleotides is favored by experimental conditions leading to a high affinity for the nucleotide and thus large levels of binding at a low nucleotide concentration. In addition, low nucleotide concentrations also are a priori favorable for binding rate measurements because rates of binding are then more likely to fall within the time-resolution range of the rapid filtration system used here. We have previously studied nucleotide binding at moderate to high concentrations of Na^+ (0.1−1M, see ref *8*), and from those data it is clear that a high ionic strength (I) results in a poor affinity for nucleotides. We therefore looked for low ionic strength conditions where the Na,K-ATPase affinity for nucleotides would be the highest, i.e., with a concentration of Na^+ high enough to induce the E_1 form of the enzyme but low enough to avoid the counterproductive effects of high ionic strength. Table 1 lists the equilibrium dissociation constants determined for ADP and ATP in the range from 7 to 157 mM Na^+. A broad minimum for K_d was found for both nucleotides in the 30−60 mM range, and we decided to work with a buffer containing 35 mM Na^+ (in the absence of monovalent cations and presence of 10 mM histidine, the equilibrium dissociation

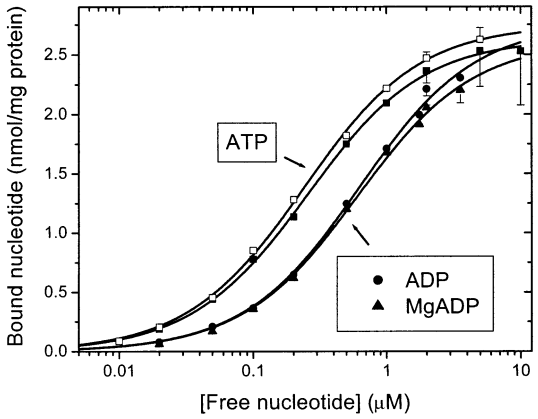

FIGURE 1: Equilibrium binding of nucleotides to Na,K-ATPase. Na,K-ATPase in 35 mM Na^+ and 10 mM histidine (pH 7.0) was equilibrated with [^{32}P]ATP (■, □) or [^{14}C]ADP (●, ▲) in the presence of 10 mM CDTA (■, □, ●) or 10 mM $MgCl_2$ (▲). The protein concentration was either 0.01 mg/mL (filled symbols) or 0.1 mg/mL (open squares). The lines through the data are hyperbolic fits with a maximal binding capacity of 2.6−2.8 nmol/mg protein and equilibrium dissociation constants for ATP of 0.25 ± 0.01 (■) or 0.24 ± 0.01 μM (□), for ADP of 0.62 ± 0.05 μM (●), and for MgADP of 0.60 ± 0.04 μM (▲).

constant for nucleotide is estimated to be much larger, namely, more than 5 μM; Fedosova and Esmann, manuscript in preparation). An additional advantage of this buffer is that the dissociation rate constant for ATP and ADP in the presence of 35 mM Na^+ (see below) is lower than that at higher concentrations (the latter was estimated to be about 13 s^{-1} for ATP at 0.1−1 M Na^+ (*8*)), presumably due to an effect of the lower ionic strength on the conformation of the ATPase. As it has already been shown that other cations such as protonated Tris induce the E_1 conformation of the enzyme in the same concentration range as Na^+ (*15*), a few experiments in the absence of Na^+ but in the presence of 35 mM Tris were also performed in the present work (see below).

When measuring binding at a very low nucleotide concentration, depletion of the nucleotide from the medium during the binding experiment must, however, be prevented. For this purpose we decided to use a low amount of protein on each filter, lower than the previously used amount of 0.1 mg protein per filter (which corresponded to about 0.28 nmol enzyme). A reduction by a factor of 10 appeared to be a good compromise in order to minimize nucleotide depletion and still allow for reliable determinations of bound radioactivity on the filter. For instance, Figure 1 shows equilibrium binding data for ATP (squares), ADP (circles), and MgADP (triangles). A low amount of protein (0.01 mg per filter) resulted in the same equilibrium dissociation constant and binding capacity (in nmol ATP bound per mg protein) as those obtained with a higher amount of protein (0.1 mg protein per filter), although the intrinsic error in bound ATP determination at the highest ATP concentrations was larger (Figure 1, compare open and filled squares; compare also the equilibrium data reported in Table 1 for experiments with 0.1 mg protein per filter with the corresponding ones in Table 2, obtained with 0.01 mg protein per filter). From the total amount of nucleotide in a volume of 40 μL, typical for the fluid wetting the filter, it can be calculated that the amount of nucleotide bound to the enzyme did not reduce the concentration of free nucleotide by more than 6% at any of the nucleotide concentrations used. Figure 1 also shows ADP and MgADP equilibrium binding under the same experimental conditions, and the affinity for these ligands is about 2-fold lower than that for ATP (see also *8*). In the presence of 35 mM Tris but absence of Na^+, the K_d's for equilibrium binding of ADP and MgADP were about 1.0 and 1.5 μM, somewhat larger than that in Na^+(not shown).

Time-Resolved Measurements of ATP Binding. Figure 2 shows the time-dependent binding of ATP at various concentrations in the presence of Na^+ and absence of Mg^{2+}. The amount of bound ATP for a given perfusion period increases with the concentration of ATP. The data were fitted by single-exponential functions, and the rate constants derived from the fits are shown in the inset to Figure 2: the observed rate constant depends on the ATP concentration in a linear fashion. This fits with a simple description of the interaction of nucleotide with Na,K-ATPase as a one-step process

$$\text{Enzyme} + \text{ATP} \rightleftarrows \text{Enzyme}\bullet\text{ATP} \qquad (1)$$

because in this case the observed rate constant for binding, k_{obs}, theoretically depends on the ATP-concentration as follows:

$$k_{obs} = k_{on}\cdot[\text{ATP}] + k_{off} \qquad (2)$$

where k_{on} is the bimolecular binding rate constant describing the reaction between Na,K-ATPase and ATP (in $\mu M^{-1}\cdot s^{-1}$) and k_{off} is the dissociation rate constant (s^{-1}). In theory, the linear fit to the data in the inset to Figure 2 allows determination of both k_{on} (from the slope) and k_{off} (from the

Table 2: Rate Constants and Equilibrium Dissociation Constants for Nucleotide and Eosin Binding to Kidney Na,K-ATPase[a]

experiment	time-resolved binding experiments (Figures 2, 5, and 7)[b]			equilibrium binding[c] (Figs. 1, 7B)	time-resolved exchange experiments (Figs. 3, 6)[d]	
ligand	k^*_{on} ($\mu M^{-1}\cdot s^{-1}$)	k^*_{off} (s^{-1})	K^*_d (calcd) (μM)	K_d (μM)	k_{off} (s^{-1})	k_{on} (calcd) ($\mu M^{-1}\cdot s^{-1}$)
ATP	11.8 ± 0.9	3.7 ±0.2	0.31	0.24 ± 0.08	7.9 ± 0.6	34
ADP	19 ± 4.4	6.3 ± 0.9	0.33	0.62 ± 0.03	14.3 ± 2.3	21
MgADP	11 ± 2.2	6.1 ± 0.5	0.55	0.61 ± 0.01	12.2 ± 1.7	20
eosin	37 ± 0.5	23 ± 0.3	0.62	0.44 ± 0.02	28 ± 3	64
	57 ± 4.7[e]	23 ± 1.6[e]	0.4[e]			

[a] The filtration experiments with nucleotides are done at 0.01 mg protein per filter at 20 °C in the presence of 35 mM Na^+ (pH 7.0). The eosin experiments are with a final protein concentration of 0.03 mg/mL. [b] Parameters derived from the time-resolved binding experiments (k^*_{on} and k^*_{off}) were obtained from linear regression analysis. K^*_d is calculated from $K^*_d = k^*_{off}/k^*_{on}$. [c] The measured equilibrium binding constant K_d is given as the average from three determinations with single-hyperbolic fits. K_d for eosin is determined from the fluorescence amplitudes of the eosin response (Figure 7B). [d] The dissociation rate constant k_{off} is given as the average from three single-exponential fits of the time-resolved exchange experiments. k_{on} is calculated from $k_{on} = k_{off}/K_d$, using the equilibrium binding determination of K_d (middle section of the table). [e] These values are deduced from eosin-dilution experiments (see text).

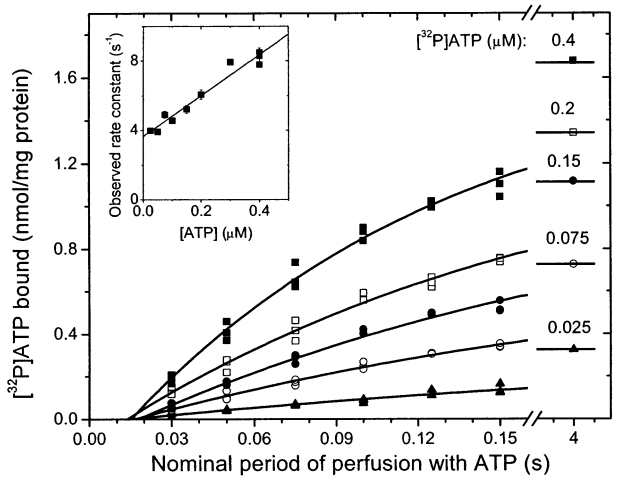

FIGURE 2: Time-resolved measurement of the binding of ATP to Na,K-ATPase. Na,K-ATPase (0.01 mg per filter) in 35 mM Na^+ and 10 mM histidine (pH 7.0) was perfused at 20 °C with [^{32}P]-ATP at concentrations of 0.4 (■), 0.2 (□), 0.15 (●), 0.075 (○), or 0.025 μM (▲) in the presence of 10 mM CDTA, and bound [^{32}P]-ATP was measured (and plotted in nmol/mg protein). The lines through the data are nonlinear least-squares fit to an exponential function of the form $y = A\cdot(1 - \exp[-k_{obs}\cdot(t - t_0)])$. Each data point represents a single determination of binding, except for the 4-second data points, which are averages of three determinations and were obtained by manual perfusion using a flow rate of about 0.5 mL/s (SD less than 10% for all points). The dead-time (t_0, the time needed for substitution of the wetting fluid in the filter) deduced from the exponential fitting in this set of experiments ranged between 14 and 18 ms. Inset: The observed rate constants (k_{obs}) are plotted as a function of the ATP-concentration and fitted according to eq 2. The fitted line has an intercept with the *y*-axis of 3.7±0.2 s^{-1}, equivalent to k^*_{off}, and a slope of 11.8±0.9 $\mu M^{-1}\cdot s^{-1}$, corresponding to k^*_{on}.

intercept with the *y*-axis): from the data in Figure 2 inset, $k^*_{off} = 3.7\ s^{-1}$ and $k^*_{on} = 11.8\ \mu M^{-1}\cdot s^{-1}$ (the parameters are asterisked to indicate that they are apparent values, deduced from the dependence of k_{obs} on the ligand concentration, see below for discussion). These values result in a computed equilibrium dissociation constant $K^*_d = k^*_{off}/k^*_{on}$ of about 0.31 μM, very close to the $K_d = 0.25\ \mu M$ derived from the equilibrium binding experiments (Figure 1). This suggests that binding of ATP indeed behaves as a simple bimolecular reaction (eq 1).

Independent Time-Resolved Measurement of the Rate of ATP Dissociation. As outlined above, the ATP-concentration dependence of k_{obs} theoretically yields both the binding and dissociation rate constant. However, it is in principle possible to experimentally determine the dissociation rate constant in a separate experiment where the enzyme is first equilibrated with radiolabeled ATP and subsequently perfused with a buffer solution without radiolabeled ATP. Such experiments were therefore performed as a control, and their results are shown in Figure 3. Unexpectedly, we found that a relatively large fraction of radiolabeled ATP remained on the filter after 1 s of perfusion when the perfusion buffer did not contain any unlabeled ATP (upper curve in Figure 3A). In contrast, inclusion of unlabeled ATP at low concentrations (5−50 μM) in the perfusion solution led to a more efficient dissociation of [^{32}P]ATP from the enzyme, as seen by the lower levels of radioactivity remaining after 1 s of perfusion (less than 10% of the initial level), without changing much the apparent rate constant for dissociation.

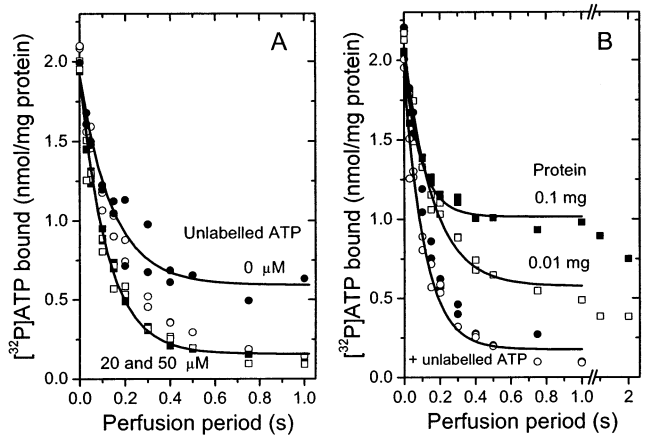

FIGURE 3: Factors important for determining the dissociation rate constant for ATP. The rate of dissociation of [(γ-^{32}P]ATP (after its binding, at an initial concentration of 1 μM, to Na,K-ATPase absorbed on a filter) was obtained by perfusing the filter for various periods with radioactivity-free buffer solution (10 mM histidine, pH 7.0, 35 mM Na^+ and 10 mM CDTA). (A) Dissociation of [^{32}P]-ATP from Na,K-ATPase (0.01 mg on filter) when the perfusion solution, in addition to buffer, contained 0 (●), 5 (○), 20 (■), or 50 μM (□) nonradioactive ATP. The data are fitted by single-exponential functions of the form $y = A\cdot\exp(-k\cdot t) + A_0$, with rate constants k of 5.9±0.5 (●), 6.9±1.1 (○, fit not shown), 8.3±0.4 (■), and 8.8±0.8 s^{-1} (□, fit not shown). The residual level of binding (A_0) was less than 10% at the higher ATP concentrations. (B) Dissociation of [^{32}P]ATP from Na,K-ATPase when the perfusion solution contained 0 (■, □) or 50 μM (●,○) nonradioactive ATP, with either 0.1 (■,●) or 0.01 mg protein on the filter (□,○). The data are fitted by single-exponential functions with rate constants of 10.6 ± 1.1(■), 6.3 ± 0.6 (□), 7.6 ± 0.4 (●, fit not shown), and 8.8 ± 0.8 s^{-1} (○).

The fraction of radioactivity remaining on the filter after 1 or 2 s of perfusion was even larger with 0.1 mg than with 0.01 mg protein on the filter (Figure 3B). In both cases, however, inclusion of unlabeled ATP in the perfusion solution effectively decreased the residual fraction of bound nucleotide after 1 s of perfusion. Thus, the results in Figure 3B suggest that the heterogeneity in dissociation kinetics in the absence of unlabeled ATP in the perfusing solution is related to the amount of binding sites for nucleotide on the filter. For 0.1 mg adsorbed protein and with an assumed wet volume of the whole filter of 30−40 μL, the actual concentration of nucleotide binding sites in the water-filled pores on the filter can be calculated to be around 10 μM, and it is even higher if the enzyme is mainly adsorbed to the upper part of the filter. With a very high affinity for ATP ($K_d \sim 0.3\ \mu M$), it is therefore possible that a fraction of the [^{32}P]-ATP dissociating from Na,K-ATPase (due to the perfusion) actually rebinds to neighboring Na,K-ATPase molecules, instead of being washed out by the perfusion solution; in this case addition of unlabeled ATP to the perfusion solution would result in isotopic dilution of the released [^{32}P]ATP, making it possible to measure a true dissociation rate constant, k_{off}. A related observation was previously made when dissociation of $^{45}Ca^{2+}$ from sarcoplasmic reticulum Ca-ATPase was measured in the absence of calcium chelator under neutral conditions, i.e., under conditions where the ATPase affinity for Ca^{2+} also is submicromolar (Champeil and Henao, unpublished results): under these conditions, rebinding of just dissociated $^{45}Ca^{2+}$ also reduced the apparent initial rate of $^{45}Ca^{2+}$ dissociation.

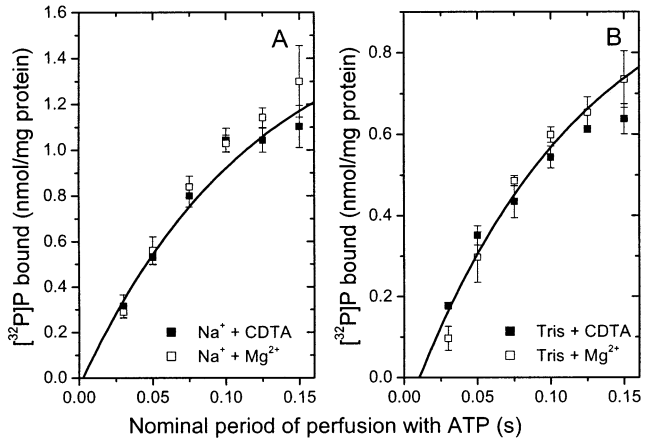

FIGURE 4: Effect of Mg^{2+} on the initial rate of binding of ATP. (A) The initial part of the binding curve at 0.4 μM ATP (cf. Figure 2, upper data set) in the presence of 10 mM CDTA (■) is compared with a similar experiment where CDTA was replaced by 10 mM $MgCl_2$ (□), with 10 mM histidine and 35 mM Na^+ present in both experiments. The line is the fit to the CDTA-data (■) previously described in the legend to Figure 2. (B) The same experiments as in panel A, but with 35 mM Tris replacing Na^+. The line is a single-exponential function with a rate constant of 8.7 s^{-1} (similar to that in panel A).

In these experiments, the rate constant for ATP dissociation, as measured with 20 or 50 μM ATP in the perfusion solution, was $k_{off} = 7-9\ s^{-1}$. Surprisingly, this value is about 2-fold larger than the value for k^*_{off} deduced from theoretical analysis of the k_{obs} versus [ligand] curve described above (inset to Figure 2). This apparent discrepancy will be discussed below.

Effect of Mg^{2+} on ATP Binding. In the presence of Mg^{2+} and Na^+, phosphorylation of the enzyme from ATP immediately follows the binding step, and a pure equilibrium binding isotherm for ATP cannot be obtained. Analysis of the initial rate of [(γ-^{32}P]ATP binding nevertheless reveals that the rate constant for MgATP binding (k_{on}) is not very different from that for Mg-free ATP: as shown by panel A in Figure 4, the initial rates of binding of ATP (at 0.4 μM ATP) were very similar in the absence and presence of 10 mM Mg^{2+} (and also at 1 mM Mg^{2+}, not shown). We also tested the effect of the presence or absence of Mg^{2+} under conditions where the divalent cation could be added without promoting phosphorylation, i.e., in the absence of Na^+ but in the presence of 35 mM Tris (to induce the E_1 form): Figure 4B shows that under these circumstances Mg^{2+} again had no strong influence on the apparent rate of binding of ATP.

Binding and Dissociation of ADP and MgADP. Experiments with ADP and MgADP similar to those for ATP were also performed, and the results are illustrated in Figures 5 and 6. For ADP (Figure 5A), extrapolation to the *y*-axis of the k_{obs} data in time-resolved binding measurements (k^*_{off}) is about 6 s^{-1}, and the slope (k^*_{on}) is about 19 $\mu M^{-1}\cdot s^{-1}$ (the K^*_d for ADP, as calculated from these rate constants, is about 0.32 μM, about half of the equilibrium value determined directly, cf. Figure 1 and Table 2); for MgADP (Figure 5B), k^*_{off} is about 6 s^{-1}, and k^*_{on} is about 11 $\mu M^{-1}\cdot s^{-1}$ (the K^*_d for MgADP calculated from these rate constants is about 0.54 μM, in fair agreement with the equilibrium value of 0.6 μM in Figure 1). The true dissociation rates for ADP and MgADP, when measured directly (Figure 6), nevertheless, seem to be again twice as high as those deduced from analysis of the k_{obs} for binding (as in the case of ATP). Note that in the case of ADP or MgADP, the presence of unlabeled nucleotide during these dissociation rate measurements (Figure 6, k_{off}) seems to be less critical than in the case of ATP, a fact that is consistent with the poorer affinity of the nucleoside diphosphate, which minimizes the rebinding artifacts suggested above to occur in the absence of unlabeled nucleotides.

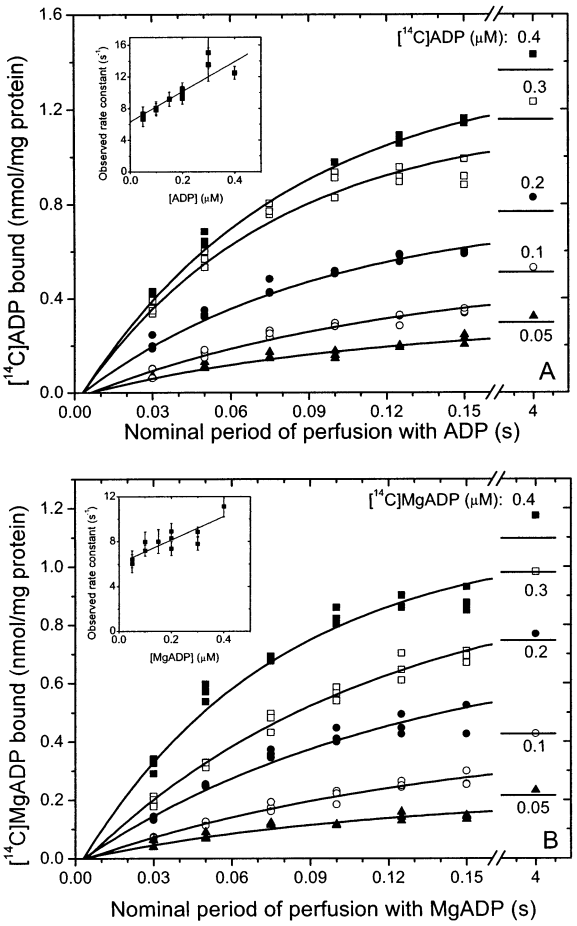

FIGURE 5: Transient kinetics of binding of ADP and MgADP to Na,K-ATPase. Na,K-ATPase (0.01 mg per filter) in 35 mM Na^+ and 10 mM histidine (pH 7.0) was perfused at 20 °C with [^{14}C]-ADP in the presence of 10 mM CDTA (panel A) or 10 mM $MgCl_2$ (panel B). The total [^{14}C]ADP concentrations were 0.4 (■), 0.3 (□), 0.2 (●), 0.1 (○), and 0.05 μM (▲), and the levels of binding are given in nmol/mg protein. Curvefits were obtained as described in the legend to Figure 2. Each data point represents a single determination of binding, except for the 4 s data points, which are averages of three determinations and were obtained by manual perfusion using a flow rate of about 0.5 mL/s (s.d. less than 15% for all points). Inset in panel A: The observed rate constants for the binding of ADP (k_{obs}) are plotted as a function of the ADP-concentrations. The linear fit has an intercept of 6.3 ± 0.9 s^{-1}, equivalent to k^*_{off}, and a slope of 19 ± 4.4 $\mu M^{-1}\cdot s^{-1}$, corresponding to k^*_{on}. Inset in panel B: The observed rate constants for the binding of MgADP (k_{obs}) are shown as a function of the MgADP concentration. The linear relationship has an intercept of 6.1 ± 0.5 s^{-1}, equivalent to k^*_{off}, and a slope of 11 ± 2.2 $\mu M^{-1}\cdot s^{-1}$, corresponding to k^*_{on}.

Binding and Dissociation Kinetics of Eosin Measured by Stopped-Flow Fluorescence. In addition to the above rapid filtration measurements with adenine nucleotides, we performed stopped-flow experiments with eosin, known to bind to the Na,K-ATPase nucleotide binding site (*14*). The

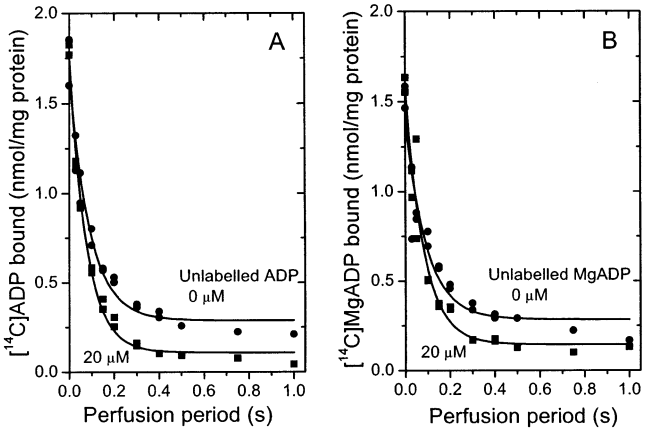

FIGURE 6: Determination of the dissociation rate constants for ADP and MgADP. [^{14}C]ADP dissociation after binding at an initial concentration of 1 μM was obtained by perfusion with buffer solution (10 mM histidine, pH 7.0, 35 mM Na^+ and 10 mM $CDTA_2$ or 10 mM $MgCl_2$). (A) Dissociation of [^{14}C]ADP from Na,K-ATPase (0.01 mg protein on filter) when the perfusion solution in addition to buffer contained 0 (●) or 20 μM (■) nonradioactive ADP. The data are fitted by single-exponential functions (see legend to Figure 3) with rate constants (k_{off}) of 11.0 ± 1.2 (●) and 13.1 ± 0.6 s^{-1} (■). The residual level of binding was about 5% with 20 μM ADP in the perfusion solution. (B) Dissociation of MgADP from Na,K-ATPase (0.01 mg protein on the filter) when the perfusion solution contained 0 (●) or 20 μM (■) nonradioactive MgADP. The data are fitted by single-exponential functions with rate constants (k_{off}) of 10.7 ± 2.0 (●) and 12.2 ± 1.7 s^{-1} (■).

interaction between eosin and Na,K-ATPase can be followed spectrofluorometrically, since the quantum yield of eosin bound to Na,K-ATPase is about 5-fold higher than that of unbound eosin (*14*). Eosin competes with ADP and ATP for binding to Na,K-ATPase, and it has been shown that the equilibrium binding constant for eosin derived from fluorescence experiments is in agreement with the observed inhibition of equilibrium ADP binding in competition experiments (*16*). In addition, the dissociation rate constant for eosin determined from stopped-flow experiments is in agreement with the ADP-induced rate of displacement of eosin (*16*). Kinetic evidence thus suggests true competition between eosin and nucleotide, and the structural homology between nucleotides and xanthene dyes such as eosin, as pointed out by Neslund et al. (*17*) and illustrated in Figure 5 in ref *14*, also suggests that eosin indeed binds to the high-affinity nucleotide binding site.

With the rapid mixing stopped-flow technique, the time-course of the reaction between eosin and Na,K-ATPase can be monitored with a time resolution that is about 1 order of magnitude faster than that of the rapid filtration technique described above. To extend the dynamic range of our monitoring of the binding/dissociation reactions at the nucleotide binding site, it was therefore of interest to examine the kinetics of eosin binding to Na,K-ATPase and see whether it conforms to an analogous simple scheme:

$$\text{Enzyme} + \text{Eosin} \rightleftarrows \text{Enzyme•eosin} \qquad (3)$$

Figure 7A shows the time-resolved increases in eosin fluorescence induced by its binding to Na,K-ATPase, as observed at various eosin concentrations. The traces were fit to monoexponential functions, and the values obtained for the amplitude of the fluorescence changes were plotted as a function of the eosin concentration in order to estimate

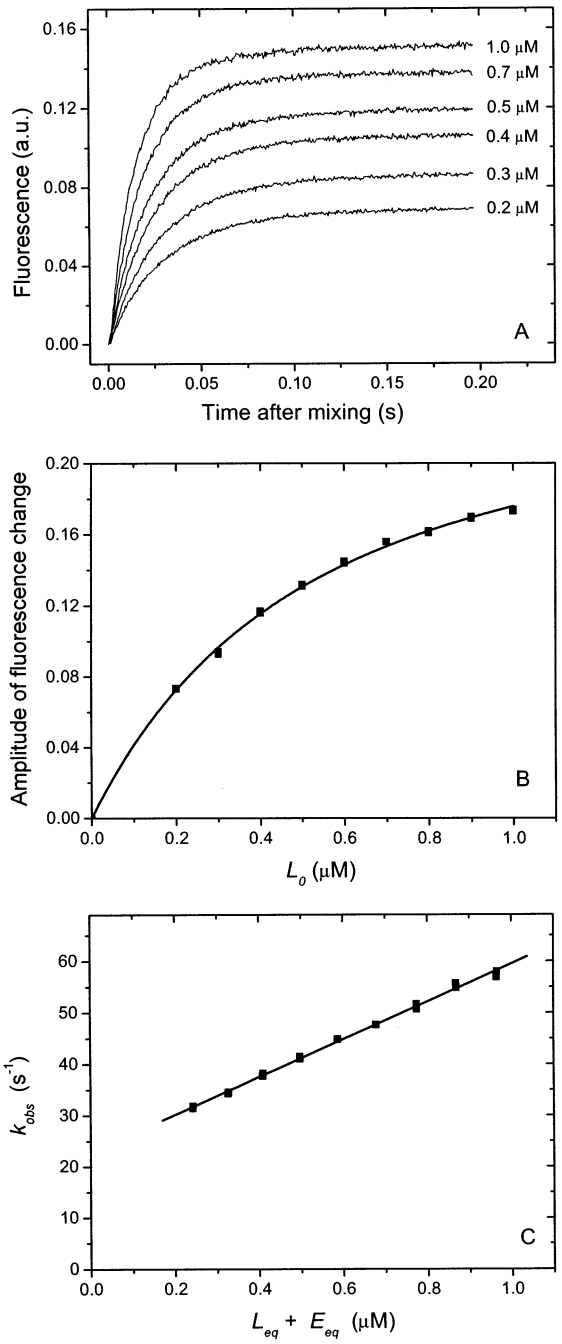

FIGURE 7: Fluorescence changes induced by eosin binding to Na,K-ATPase. Na,K-ATPase in 35 mM Na^+, 10 mM CDTA and 10 mM histidine (pH 7.0) was mixed with eosin (final concentrations were 0.1 μM for Na,K-ATPase and 0.2, 0.3, 0.4, 0.5, 0.7, and 1 μM for eosin). (A) Typical fluorescence traces. (B) Amplitude of the fluorescence change as function of total eosin concentration (L_0). The data from 3 independent titrations were fitted to eq 4 (see text). The calculated K_d value (eq 4) is 0.44 ± 0.02 μM. (C) k_{obs} as a function of the sum of the equilibrium concentrations of eosin (L_{eq}) and enzyme (E_{eq}, see text). The slope of the straight line and its intercept with the *y*-axis (eq 5) give the values of $k^*_{on} = 37 \pm 0.5$ $\mu M^{-1}\cdot s^{-1}$ and $k^*_{off} = 23 \pm 0.3$ s^{-1}.

the ATPase affinity for eosin, cf. Figure 7B. Examination by eye suggested a submicromolar equilibrium dissociation constant, in the 0.3−0.6 μM range. However, since the total concentration of enzyme was 0.1 μM in this experiment, i.e., on the same order of magnitude as the lowest concentrations of eosin tested, the concentration of free eosin must have changed slightly during the binding reaction. Hence, a

somewhat more elaborate analysis of these amplitude data was adopted, taking into account the fact that the equilibrium concentrations of the free and bound forms of enzyme obey a classical quadratic equation. The data in Figure 7B were thus fitted to the following equation:

$$F = F_{max}\cdot\{E_0 + L_0 + K_d - [(E_0 + L_0 + K_d)^2 - 4\cdot E_0\cdot L_0]^{1/2}\}/(2\cdot E_0) \quad (4)$$

where F_{max} is the maximal change in the fluorescence, E_0 is the total enzyme concentration (0.1 μM), L_0 is the total eosin (ligand) concentration, and K_d is the equilibrium dissociation constant for eosin. Curve fitting of the data in Figure 7B resulted in $K_d = 0.44$ μM. The fraction of eosin bound was calculated to range between 14% (at $L_0 = 0.2$ μM) and 6% (at $L_0 = 1.0$ μM), showing that the concentration of free eosin indeed does vary during the binding reaction, but only to a minor extent, which explains why the time-dependence of the fluorescence changes could be fitted to single exponential functions fairly well.

To estimate the rate constants for binding and dissociation of eosin from the observed rate constants (k_{obs}) in the above experiments, these observed rate constants could conceivably have been plotted against the total eosin concentration, as we have done in the case of ATP and ADP. However, again as the enzyme concentration is on the same order of magnitude as the lower eosin concentrations, a somewhat more elaborate procedure was adopted. In fact, such conditions are classical in chemical relaxation studies (*18*), and studies have already shown that under these conditions rate constants for ligand binding or dissociation are best estimated by plotting observed rates as a function of the sum of enzyme and ligand concentrations, both at equilibrium:

$$k_{obs} = k_{on}\cdot(E_{eq} + L_{eq}) + k_{off} \quad (5)$$

In Figure 7C, k_{obs} was therefore plotted against the sum of the equilibrium values for ligand and enzyme (L_{eq} and E_{eq}, as calculated from the above-estimated K_d), rather than against the total ligand concentration (L_0). The slope of the straight line and its intercept with the *y*-axis give the values of $k^*_{on} = 37$ $\mu M^{-1}\cdot s^{-1}$ and $k^*_{off} = 23$ s^{-1}. This leads to a calculated value of $K^*_d = k^*_{off}/k^*_{on} = 0.62$ μM, in reasonable agreement with 0.44 μM determined from the amplitude data of Figure 7B.

The observed rate constants were also measured in other concentration jump experiments, where preequilibrated eosin−enzyme complexes were diluted 2-fold with buffer and the approach to a new equilibrium was again followed fluorometrically. The single-exponential decays in eosin fluorescence due to dissociation of the eosin−enzyme complexes provided a k_{obs} value for each value of the initial eosin concentration (not shown). Analysis of the data in the same way as above resulted in the following values for k^*_{on} and k^*_{off} for eosin binding: $k^*_{on} = 57$ $\mu M^{-1}\cdot s^{-1}$, $k^*_{off} = 23$ s^{-1}, leading to a calculated K^*_d of 0.40 μM in close agreement with 0.44 μM determined from the amplitude data of Figure 7B.

In additional dilution experiments we found that the presence of 200 μM ADP in the second syringe induced complete dissociation of eosin from the binding site (not shown); in this case the observed decrease in fluorescence was described by a single-exponential function with a rate constant of 28 s^{-1} (dissociation rate constant k_{off} for eosin). Thus, in the case of eosin measurements, the value deduced from exchange experiments (k_{off}) is consistent with the one deduced from the ligand dependence of the observed rate constant measured in binding reactions (k^*_{off}). Calculation of $k_{on} = k_{off}/K_d$, using $K_d = 0.44$ μM, results in a value of 64 $\mu M^{-1}\cdot s^{-1}$.

In Table 2 all experimentally determined parameters (Figures 2−7) are collected, as well as computed ones.

DISCUSSION

Our interpretation of the data presented in this work is that the binding and dissociation of nucleotide essentially follows a simple model. This conclusion is based on the observation that the observed rate constant for nucleotide binding depends linearly on the nucleotide concentration in the experimentally accessible range, cf. Figure 2, inset, and the ratio between "ON" and "OFF" rate constants for nucleotide binding to the Na,K-ATPase extracted from the time-resolved binding experiment agrees with the equilibrium dissociation constant of these ligands (cf. insets to Figures 2 and 5), i.e., $K^*_d = k^*_{off}/k^*_{on}$. In addition, we show that the presence of Mg^{2+} does not change the kinetics of the initial nucleotide binding step.

In the rapid filtration experiments, the off-rate constant deduced from analysis of time-resolved binding experiments (k^*_{off}) is about 2-fold slower than the dissociation rate constant directly measured in an exchange reaction (k_{off}). It therefore appears that with these membrane fragments, the rapid filtration experimental setup imposes some apparent slowing of the binding process. After considering and discarding a number of other possibilities, we suggest here that the binding sites in Na,K-ATPase membrane fragments (sheets) adsorbed on the filters are not equally accessible to perfusion solution. In a naive picture, the cytoplasmic side of the adsorbed membranous ATPase sheets can indeed be facing either the nitrocellulose wall of the filter pore or the solution itself. If, for example, half of the enzyme molecules are relatively inaccessible, the initial rates of binding will correspond to binding to only half of the ATPase molecules present, although for long incubation periods even ATPases oriented in an unfavorable manner will have time to equilibrate with ATP. This will lead to underestimates of all k_{obs} values and therefore would diminish both the extracted k^*_{on} (the slope) and k^*_{off} (the intercept with the *y*-axis); in addition, binding kinetics over long periods of perfusion may deviate from strictly single-exponential behavior. Such heterogeneity in ATPase sites will also manifest itself in dissociation experiments, but less so in the presence of the excess of unlabeled nucleotide, i.e., in "exchange" experiments. Note that such an artifact is likely not to manifest itself with closed vesicular membrane preparations such as sarcoplasmic reticulum vesicles (with binding sites on the external surface), where the fraction of the vesicle surface in contact with the pore walls is small, but is likely to become significant indeed in the case of open membranous sheets such as Na,K-ATPase membranes.

If this interpretation is valid, the correct off-rate constants are those (k_{off}) determined directly in dissociation experiments in the presence of unlabeled nucleotide (Figures 3 and 6) rather than those (k^*_{off}) deduced from extrapolation of k_{obs}

values to the *y*-axis (insets in Figures 2 and 5), and the correct on-rate constants (k_{on}) are larger than those deduced from the ligand dependence of k_{obs} (k^*_{on}): these correct on-rate constants are more reliably estimated by computing them from k_{off} and K_d. Interestingly, in the case of fluorescence spectroscopy experiments with eosin, we find a fair agreement between the kinetic parameters deduced from either time-resolved binding or time-resolved exchange experiments (cf. Table 2): this is probably derived from the fact that in stopped-flow fluorescence studies, in contrast to rapid filtration studies, there is no concern about heterogeneity of the binding sites regarding their accessibility.

The k_{on} values of 20−40 $\mu M^{-1}\cdot s^{-1}$ estimated here for nucleotide binding to Na,K-ATPase are on the same order of magnitude as those previously estimated for the same bimolecular rate constant in case of the closely related sarcoplasmic reticulum Ca-ATPase. For binding at the nucleotide site of this ATPase of the CaATP complex, rapid filtration experiments similar to those described here had suggested a k_{on} value of about 4 $\mu M^{-1}\cdot s^{-1}$ at pH 7 and 5 °C (in the absence of Mg^{2+}) (*19*), and a similar value was found for MgATP binding (in the presence of Ca^{2+} and Mg^{2+}), again at pH 7 and 5 °C (see ref *20*). For Ca-ATPase, a k_{on} value of about 10 $\mu M^{-1}\cdot s^{-1}$ was also deduced from phosphorylation measurements performed by quenched flow at 25 °C (pH 7) in the presence of Mg^{2+} (*21*). In the case of Na,K-ATPase, a similar estimate for MgATP can in fact also tentatively be derived from phosphorylation time courses observed in quenched flow experiments. For instance, in the presence of 5 μM ATP, the observed rate constant for phosphorylation was found to be about 3000 min^{-1}, i.e., 50 s^{-1}, while at saturating ATP concentration it was about 200 s^{-1} (*22*; see also refs *23* and *24*). Accepting the fair hypothesis that at low concentrations of ATP the rate of phosphorylation is limited by ATP binding itself, this would suggest that the binding of 5 μM MgATP occurs with a k_{obs} of 50 s^{-1}, i.e., the "k_{on}" rate constant for MgATP would be of the order of about 10 $\mu M^{-1}\cdot s^{-1}$, similar to the one measured here directly. For nucleotide analogues FDP and FTP, Karlish et al. (*25*) determined equilibrium dissociation and dissociation rate constants, from which binding rate constants for both nucleotides were deduced to be about 30 $\mu M^{-1}\cdot s^{-1}$, again in close agreement with the values obtained here (Table 2).

Thus, the nucleotide binding to Na,K-ATPase is adequately described, on the millisecond time scale of the present experiments, as a single-step event with binding rate constants of about 20−40 $\mu M^{-1}\cdot s^{-1}$. On the other hand, determination of the structure of Ca-ATPase at the atomic level (*26*, *27*) in two different conformations has recently suggested that a major rearrangement of domains in the cytoplasmic part of the protein was occurring as a consequence of nucleotide binding. If such an event is part of the Na,K-ATPase reaction with ATP (prior to phosphorylation), our data imply that this rearrangement of domains in Na,K-ATPase must be rapid: if binding was followed by some slow step, this would probably be revealed by a biphasic binding time course, while considering the time resolution of our filtration experiments (whose effective dead time is about 10−20 ms, the time needed to replace the filter wetting volume), fast conformational rearrangements after binding would certainly remain undetected if they were occurring on the submillisecond time scale. This places a lower limit on the putative rate of reorganization of the cytosolic domains (note that from the start, the rate of such a putative reorganization has been considered to be fast and only dependent on Brownian motion, see ref *26*). Alternatively, the widely open "E_1" structure obtained for Ca-ATPase crystallized in the presence of Ca^{2+} (*26*) might be an extreme but rare conformation, or such a widely open structure might not be prominent with Na,K-ATPase. Another possibility would be that the putative domain movement has little or no effect on the accessibility of the adenine-binding site.

ACKNOWLEDGMENT

The excellent technical assistance of Ms. Angielina Damgaard and Ms. Birthe Bjerring Jensen is acknowledged.

REFERENCES

1. Møller, J. V., Juul, B., and le Maire, M. (1996) *Biochim. Biophys. Acta 1286*, 1−51.
2. Hegyvary, C., and Post, R. L. (1971) *J. Biol. Chem. 246*, 5234−5240.
3. Nørby, J. G., and Jensen, J. (1971) *Biochim. Biophys. Acta 233*, 104−116.
4. Cantley, L. C., Jr., Gelles, J., and Josephson, L. (1978) *Biochemistry 17*, 418−425.
5. Moczydlowski, E. G., and Fortes, P. A.(1981) *J. Biol. Chem. 256*, 2346−2356.
6. Klodos, I., Esmann, M., and Post, R. L (2002) *Kidney Intl. 62*, 2097−2100.
7. Jørgensen, P. L. (1975) *Biochim. Biophys. Acta 356*, 36−52.
8. Fedosova, N. U., Champeil, P., and Esmann, M. (2002) *Biochemistry*, *41*, 1267−1273.
9. Dupont, Y. (1980) *Eur. J. Biochem. 109*, 231−238.
10. Champeil, P., and Guillain, F. (1986) *Biochemistry 25*, 7623−7633.
11. Dupont, Y. (1984) *Anal. Biochem. 142*, 504−10.
12. Champeil, P., Riollet, S., Orlowski, S., Guillain, F., Seebregts, C. J., and McIntosh, D. B. (1988) *J. Biol. Chem. 263*, 12288−12294.
13. Hannaert-Merah, Z., Coquil, J. F., Combettes, L., Claret, M., Mauger, J. P. and Champeil, P. (1994) *J. Biol. Chem. 269*, 29642−29649.
14. Esmann, M., and Fedosova, N. U. (1997) *Ann. N.Y. Acad. Sci. 834*, 310−321.
15. Skou, J. C., and Esmann, M. (1980) *Biochim. Biophys. Acta 601*, 386-402.
16. Esmann, M. (1992) *Biochim. Biophys. Acta 1110*, 20−28.
17. Neslund, G. G., Miara, J. E., Kang, J.-J. and Dahms, A. S. (1984) *Cell Regul. 24*, 447−468.
18. Ruf, H., and Grell, E. (1981) *Mol. Biol. Biochem. Biophys. 31*, 333−376.
19. Lacapère, J. J., and Guillain, F. (1990) *J. Biol. Chem. 265*, 8583−8589.
20. Lacapère, J. J., and Guillain, F. (1993) *Eur. J. Biochem. 211*, 117−126.
21. Petithory, J. R., and Jencks, W. P. (1988) *Biochemistry 27*, 5553−5564.
22. Mårdh, S., and Zetterquist, Ö. (1974) *Biochim. Biophys. Acta 350*, 473−483.
23. Hobbs, A. S., Albers, R. W., and Froehlich, J. P. (1988) in *The Na^+,K^+-Pump, Part A, Molecular Aspects* (Skou, J. C., Nørby, J. G., Maunsbach, A. B., and Esmann, M., Eds.) pp 307−314, Alan R. Liss, Inc., New York.
24. Kane, D., Fendler, K., Grell, E., Bamberg, E., Taniguchi, K., Froehlich, J. P., and Clarke, R. J. (1997) *Biochemistry 36*, 13406−13420.
25. Karlish, S. J. D., Yates, D. M., and Glynn, I. M. (1978) *Biochim. Biophys. Acta* 525, 230−251.
26. Toyoshima, C., Nakasako, M., Nomura, H., and Ogawa, H. (2000) *Nature 405*, 647−655.
27. Toyoshima, C., and Nomura, H. (2002) *Nature 418*, 605−611.

BI0268302